Journal of Orthopaedic Surgery and Research

RESEARCH ARTICLE

Open Access

Modulating tumor-associated macrophage polarization by anti-maRCO mAb exerts anti-osteosarcoma effects through regulating osteosarcoma cell proliferation, migration and apoptosis

Lei Ding[1†], Ling Wu[2†], Yuting Cao[3†], Hao Wang[2], Defang Li[1], Weibin Chen[1], Ping Huang[2*] and Zengxin Jiang[3*]

Abstract

Purpose Osteosarcoma is a primary bone tumor lacking optimal clinical treatment options. Tumor-associated macrophages in the tumor microenvironment are closely associated with tumor development and metastasis. Studies have identified the macrophage receptor with collagenous structure (MARCO) as a specific receptor expressed in macrophages. This study aimed to investigate whether anti-MARCO mAb treatment can induce macrophage polarization in the tumor microenvironment and elicit anti-tumor effects.

Methods THP-1 cells were treated with 20 ng/mL phorbol 12-myristate 13-acetate and 80 ng/mL interleukin-4 for 48 h to induce macrophage polarization to alternatively activated macrophages (M2). Enzyme-linked immunosorbent assay, real-time quantitative polymerase chain reaction, flow cytometry, and bioinformatic analyses were performed to evaluate macrophage polarization. The co-culture groups included a blank group, an M2 macrophage and U2OS co-culture group, and an anti-MARCO mAb-treated M2 macrophage group. Cell viability assays, cell scratch tests, apoptosis, and cell cycle analyses were performed to determine the effects of anti-MARCO mAb-treated macrophages on osteosarcoma cells.

Results It was demonstrated that anti-MARCO mAb can drive macrophages toward classically activated macrophage (M1) polarization. Anti-MARCO mAb promoted the secretion of pro-inflammatory factors by macrophages, including tumor necrosis factor-alpha (TNF-α), interleukin-1beta, interleukin-6 and interleukin-23. Studies on in vitro co-culture models have revealed that macrophages treated with anti-MARCO mAb can suppress the growth and migration of osteosarcoma cells, induce cell apoptosis, and inhibit cell cycle progression of osteosarcoma cells through M1 polarization of macrophages in vitro.

†Lei Ding, Ling Wu and Yuting Cao contributed equally to this work.

*Correspondence:
Ping Huang
305836@hospital.cqmu.edu.cn
Zengxin Jiang
Dr_Jiangzx@163.com

Full list of author information is available at the end of the article

Conclusion Anti-MARCO mAb treatment exerts anti-osteosarcoma effects by affecting macrophage polarization toward M1 macrophages, offering a potential new therapeutic approach for treating osteosarcoma.

Keywords Macrophage, MARCO, Osteosarcoma, Co-culture, Polarization

Introduction

Osteosarcoma is the most common invasive bone tumor, accounting for approximately 20% of all bone tumors [1, 2], and occurs mostly in adolescents and adults older than 60 years [3]. It predominantly develops in the epiphysis of the long bones [4]. Despite the introduction of chemotherapy for osteosarcoma treatment in the 1970s, the 5-year event-free survival rate for patients with non-metastatic osteosarcoma has reached 60%. However, 60–70% of patients with osteosarcoma experience lung metastasis, leading to a 5-year event-free survival rate of less than 40%. Especially in patients with early lung metastasis, the 5-year event-free survival drops below 20% [5–7]. Consequently, new research on treatment methods has become a prominent subject in basic and clinical research [8]. Immune checkpoint therapy, an emerging clinical approach, has proven effective in treating numerous malignancies [9]. However, approved immune checkpoint therapies, including programmed cell death ligand 1 (PD-L1), show poor efficacy in osteosarcoma patients [10]`. Therefore, novel therapeutic targets need to be identified.

The tumor microenvironment (TME), a specialized, complex, and highly dynamic mixture comprising diverse immune cells, is believed to contribute to the development and metastasis of osteosarcoma [11]. Consequently, further understanding of the TME may facilitate elucidation of the mechanisms underlying osteosarcoma metastasis and identification of new treatment targets. Currently, tumor-associated macrophages (TAMs) have drawn researchers' attention as macrophages recruited to the TME, constituting 30–50% of inflammatory cells in the TME and closely correlating with tumor cell proliferation, invasion, and metastasis [12, 13]. TAMs primarily exist in two polarized phenotypes, classically activated macrophages (M1) and alternatively activated macrophages (M2), which have different functions in immune defense and surveillance and can be interconverted [14]. TAMs are more polarized toward M2 macrophages, which are believed to promote tumor occurrence and metastasis [15, 16]. M1 macrophages have anti-tumor effects in various ways, including releasing tumor-killing molecules to kill tumor cells [17], maintaining an inflammatory state, and enabling the immune system to detect and engulf tumor cells [18]. Therefore, promoting the polarization of macrophages toward M1 macrophages and inhibiting M2 macrophages is considered a feasible anti-tumor strategy.

Based on this background, researchers have assessed the clinical viability of various macrophage markers in TAMs [19]. Macrophage receptors with collagenous structure (MARCO), a pattern recognition receptor belonging to the class A scavenger receptor family, are overexpressed in the TME [20]. It has been identified to define a subtype of inhibitory TAM and is associated with clinical outcomes [21, 22]. Previous research has discovered an anti-MARCO mAb and demonstrated its anti-tumor effects in mouse breast cancer, colon cancer, and melanoma models [23]. However, its potential role in osteosarcoma treatment remains unknown. Consequently, we conducted this study to explore whether anti-MARCO mAb could similarly induce polarization in human macrophages in the TME of osteosarcoma, thereby exerting anti-tumor effects in osteosarcoma.

Materials and methods

Cell culture

THP-1 (RRID: CVCL_0006) and U2OS cells (RRID: CVCL_0042) were purchased from the Cell Bank of the Chinese Academy of Sciences (Shanghai, China). Differentiation into macrophages was induced using 20 ng/mL phorbol 12-myristate 13-acetate (PMA; Sigma-Aldrich, MO, USA). Macrophage polarization to M2 macrophages was induced by treating THP-1 cells with 20 ng/mL PMA and 80 ng/mL interleukin-4 (IL-4, Sigma-Aldrich, USA) for 48 h. The cells were cultured in RPMI-1640 medium (Gibco; Thermo Fisher Scientific Inc., MA, USA) supplemented with 10% fetal bovine serum (Gibco; Thermo Fisher Scientific Inc.) with 5% CO_2 at 37 °C. Cells were plated in 6-well or 96-well plates for subsequent experiments. For the co-culture experiments, the groups included a blank group, M2 macrophages and U2OS co-culture group, and anti-MARCO mAb-treated M2 macrophage group (anti-MARCO mAb 2 μg/mL). Transwells (Corning, NY, USA) with a 0.4 μm aperture were used for co-culture experiments. Co-culture was initiated when macrophages were treated with anti-MARCO mAb for 48 h. Macrophages were cultured in the upper chamber, and U2OS cells were cultured in the lower chamber. After culturing for the indicated times, the cells were harvested for subsequent assays.

Cell viability

Cell viability was assessed using the Cell Counting Kit-8 (CCK-8) assay kit (DOJINDO, Kumamoto, Japan). Cells were seeded in 96-well plates (4000 cells/well) and treated with anti-MARCO mAb (0.5, 1, 2, 5, 10, and 20 μg/mL;

Cat No. MA1-40315, Thermo Fisher Scientific Inc.) for 24 and 48 h. U2OS cells were seeded in 96-well plates (4000 cells/well) and co-cultured with macrophages. Cells were washed twice with phosphate-buffered saline (PBS, Gibco) and then incubated with serum-free 1640 medium containing 10% CCK-8 at 37 °C for 2 h. The optical density of each well was measured at 450 nm using a microplate reader (Epoch; BioTek Instruments, Inc., Winooski, VT, USA).

Real-time quantitative polymerase chain reaction (RT-qPCR)

RT-qPCR analysis was performed to detect the mRNA expression of inducible nitric oxide synthase (iNOS), Arginase-1 (Arg-1) and cluster of differentiation 206 (CD206) after treatment with anti-MARCO mAb. Glyceraldehyde-3-phosphate dehydrogenase (GAPDH) was used as the internal reference. Total RNA was extracted using a Universal RNA Purification Kit (EZBioscience, MN, USA), followed by reverse transcription using 4× EZscript Reverse Transcription Mix (EZBioscience). Subsequently, cDNA was subjected to qPCR using 2× EZ COLOR SYBR GREEN QPCR MASTER MIX (EZBioscience) on a LightCycler 480 II instrument. The reaction mixture comprised 5 μL of 2× EZ COLOR SYBR GREEN QPCR MASTER MIX, 0.4 μL of primer working solution, 0.2 μL of template DNA, and 4.4 μL of diethylpyrocarbonate-treated water. The thermocycling conditions were as follows: initial denaturation at 95 °C for 5 min, followed by 40 cycles of denaturation at 95 °C for 10 s, annealing/extension at 60 °C for 30 s, and final melting curve collection at 95 °C for 15 s, 60 °C for 1 min, and 95 °C for 30 s. The data were normalized to GAPDH as an internal reference, and the relative expression levels were analyzed using the 2-ΔΔCt method. Primer sequences are listed in Table 1.

Flow cytometric analysis

The cells were washed twice with PBS and then added to 100 μL CD86 solution diluted in NCM universal antibody diluent (NCM Biotech Co., Ltd. Suzhou, China; 1:100). The mixture was then incubated on ice for 15 min, followed by washing. The True-Nuclear™ Transcription Factor Buffer Set (BioLegend, San Diego, CA, USA) was employed for cell membrane permeabilization. First, 1 mL of True-Nuclear Fix buffer (1×; BioLegend) was added and incubated in the dark at room temperature for 45 min. Then, 2 mL of True-Nuclear Perm Buffer (1×; BioLegend) was added, centrifuged, and the supernatant was discarded. Subsequently, 2 mL of True-Nuclear Perm Buffer with a 1:100 dilution of CD206 antibody (RRID: AB_2573182) and a 1:200 dilution of CD86 antibody (RRID: AB_10372961) were added, followed by incubation on ice for 15 min. After centrifugation, the supernatant was discarded, and the cells were resuspended in PBS. Flow cytometry (CytoFLEXLX; Beckman Coulter, Inc., CA, USA) was used for detection.

Table 1 Primers' sequences used in the real-time PCR (5′ – 3′)

Gene	Forward (5′-3′)	Reverse (5′-3′)
iNOS	TCCGAGGCAAACAGCACATTCA	GGGTTGGGGGT GTGGTGATGT
Arg-1	TGGACAGACTAGGAATTGGCA	CCAGTCCGTCAA CATCAAAACT
CD206	TACAAAAGTGACATGCCTCAGTT	TGTGTAGAGTATA GAGGGGCAGA
GAPDH	ACAACTTTGGTATCGTGGAAGG	GCCATCACGCCA CAGTTTC

iNOS, inducible nitric oxide synthase; Arg-1, Arginase-1; CD206, cluster of differentiation 206; GAPDH, glyceraldehyde-3-phosphate dehydrogenase

Bioinformatics analysis

After treating the cells with 2 μg/mL anti-MARCO mAb for 48 h, total RNA was extracted from macrophages using TRIzol reagent (Invitrogen, Carlsbad, CA, USA). Transcriptome sequencing were performed by Oebiotech (Shanghai, China). Sequencing was performed using an Illumina HiSeq 2500 platform. Differential expressed genes (DEGs) analysis was conducted using the DEseq2 package (1.34.0). Genes with a p-value < 0.05 and |log2 (foldchange)| ≥ 0.58 were considered DEGs. Gene ontology (GO) and Kyoto encyclopedia of genes and genomes (KEGG) analyses were performed for DEGs using the DAVID tool ((http://david.abcc.ncifcrf.gov/). Results with p < 0.05 were retained. Gene set enrichment analysis (GSEA) was performed using GSEA software v3.0 (Broad Institute, MIT, USA). Significance was set at a false discovery rate (q value) < 0.25 and p-value < 0.05.

Enzyme-linked immunosorbent assay (ELISA)

ELISA kits (NeoBioscience Technology Co., Ltd., Shenzhen, China) were used to measure the secretion of tumor necrosis factor-alpha (TNF-α), IL-1β, IL-6, and IL-23 from cells. First, the supernatant was collected, samples or standards (100 μL) were added to each well, and the plate was sealed and incubated at 37 °C in the dark for 90 min. The plate was washed, a biotinylated antibody working solution (100 μL) was added, and the plate was sealed and incubated at 37 °C in the dark for 60 min. Then again, the plate was washed, enzyme conjugate working solution (100 μL) was added, and incubated at 37 °C in the dark for 30 min. Again, the plate was washed, 100 μL color substrate was added and incubated at 37 °C in the dark for 15 min, and 100 μL stop solution was added. The optical density was measured at 450 nm using a microplate reader (Epoch; BioTek Instruments, Inc.), and the concentrations of TNF-α, IL-1β, IL-6, and IL-23 were calculated based on a standard curve.

Cell scratch test

First, lines were drawn on the back of a six-well plate. After 24 h of cell culture, two parallel lines perpendicular to the drawn lines were scratched using a 10 μL pipette tip. The detached cells were washed away, and after 48 h of incubation, they were observed under a microscope at the same positions before and after treatment. The scratch healing area was calculated using Image J 1.8.0 software (National Institutes of Health, USA) with the formula: Healing Percentage = (Initial Scratch Area − Final Scratch Area)/Initial Scratch Area × 100.

Cell apoptosis analysis

Cell apoptosis was examined using an Annexin V-FITC/PI dual staining kit (BD Biosciences, USA). The process involved washing cells twice with PBS, resuspending cells in 300 μL Binding Buffer (1×), adding 5 μL Annexin V-FITC, incubating in the dark at room temperature for 25 min, adding 5 μL PI, incubating in the dark at room temperature for 5 min, then adding 200 μL 1× Binding Buffer. The chondrocyte apoptotic rate was measured using flow cytometry (CytoFLEXLX; Beckman Coulter, Inc.).

Cell cycle detection

Cell cycle detection was conducted using a Tali™ Cell Cycle Kit (Thermo Fisher Scientific, Inc.). Cells were washed twice with PBS, resuspended in 200 μL of Tali® Cell Cycle Solution, and incubated in the dark at room temperature for 30 min. FlowJo software (version 10.0; FlowJo, LLC, Ashland, OR, USA) was used for analysis.

Data analysis

Each experiment was conducted independently three times, and the data are presented as mean ± stand deviation (SD). Normally distributed data were analyzed using the Shapiro–Wilk test. The Student's *t*-test was used to compare the two groups. Statistical comparisons among multiple groups were performed using one-way analysis of variance (ANOVA), followed by Bonferroni's multiple comparison test. $p < 0.05$ was considered statistically significant. Statistical Package for the Social Sciences (SPSS, version 22.0; IBM Corp, Armonk, NY, USA) was used for all statistical analyses.

Results

Anti-MARCO mAb induced macrophage polarization toward M1 macrophages

The impact of the anti-MARCO mAb on macrophage cell activity was evaluated using the CCK8 assay. No significant effect on cell activity was observed in vitro after 24 and 48 h of treatment with 0.5, 1, 2, 5, 10, and 20 μg/mL of anti-MARCO mAb, suggesting that anti-MARCO mAb does not have cell toxicity (Fig. 1A-B). Subsequently, the effect of the anti-MARCO mAb on macrophage polarization was evaluated. RT-qPCR analysis revealed that 0.5, 1, 2, and 5 μg/mL of anti-MARCO mAb increased iNOS expression in macrophages, peaking at 2 μg/mL (Fig. 1C). Additionally, 0.5, 1, 2, and 5 μg/mL of anti-MARCO mAb decreased the expression of Arg-1 and CD206, reaching a minimum at 2 μg/mL (Fig. 1D–E). The results disclosed that anti-MARCO mAb promoted macrophage polarization toward M1 macrophages. Flow cytometry analysis revealed that 2 μg/mL anti-MARCO mAb increased CD86 expression levels and decreased CD206 expression levels in macrophages (Fig. 1F–H), consistent with RT-qPCR results, confirming that anti-MARCO mAb induces macrophage polarization toward M1 macrophages.

Anti-MARCO mAb promoted pro-inflammatory cytokine secretion by macrophages

To further explore the effect of anti-MARCO mAb on macrophages, transcriptome RNA analysis was performed on the anti-MARCO mAb-treated macrophages and the control group. The heatmap and volcano plot show significant differences in gene expression (Fig. 2A–B). Gene enrichment analysis was conducted. Biological process (BP), cellular component (CC), and molecular function (MF) analyses of differentially expressed genes revealed significant differences between anti-MARCO mAb-treated and control groups. The top ten terms are presented in Fig. 3A–F. KEGG pathway analysis showed a concentration of differences in inflammation-related pathways, with the top 10 terms displayed in Fig. 3G–H. Gene set enrichment analysis was also performed. The pathways with significant differences in the HALLMARK pathway analysis results are displayed in Fig. 4. Compared with the control group, there was a significant increase in the expression of inflammatory and TNF-α-related gene sets in the anti-MARCO mAb group (Fig. 4A and C). The mRNA expression of several significant pro-inflammatory cytokines associated with anti-tumor activity, including TNF-α, IL-1β, IL-6, and IL-23, was elevated in the anti-MARCO mAb group (Fig. 5A). RNA-seq expression data are presented in supplementary file (Supplement 1). Additionally, ELISA analysis further confirmed significantly higher secretion levels of TNF-α, IL-1β, IL-6, and IL-23 in the anti-MARCO mAb-treated group than in the control group (Fig. 5B–E). These findings are consistent with the bioinformatics results, demonstrating that anti-MARCO mAb enhances macrophage polarization toward M1 and increases pro-inflammatory cytokine secretion. This further supports our hypothesis that macrophages tend to polarize toward pro-inflammatory M1 macrophages.

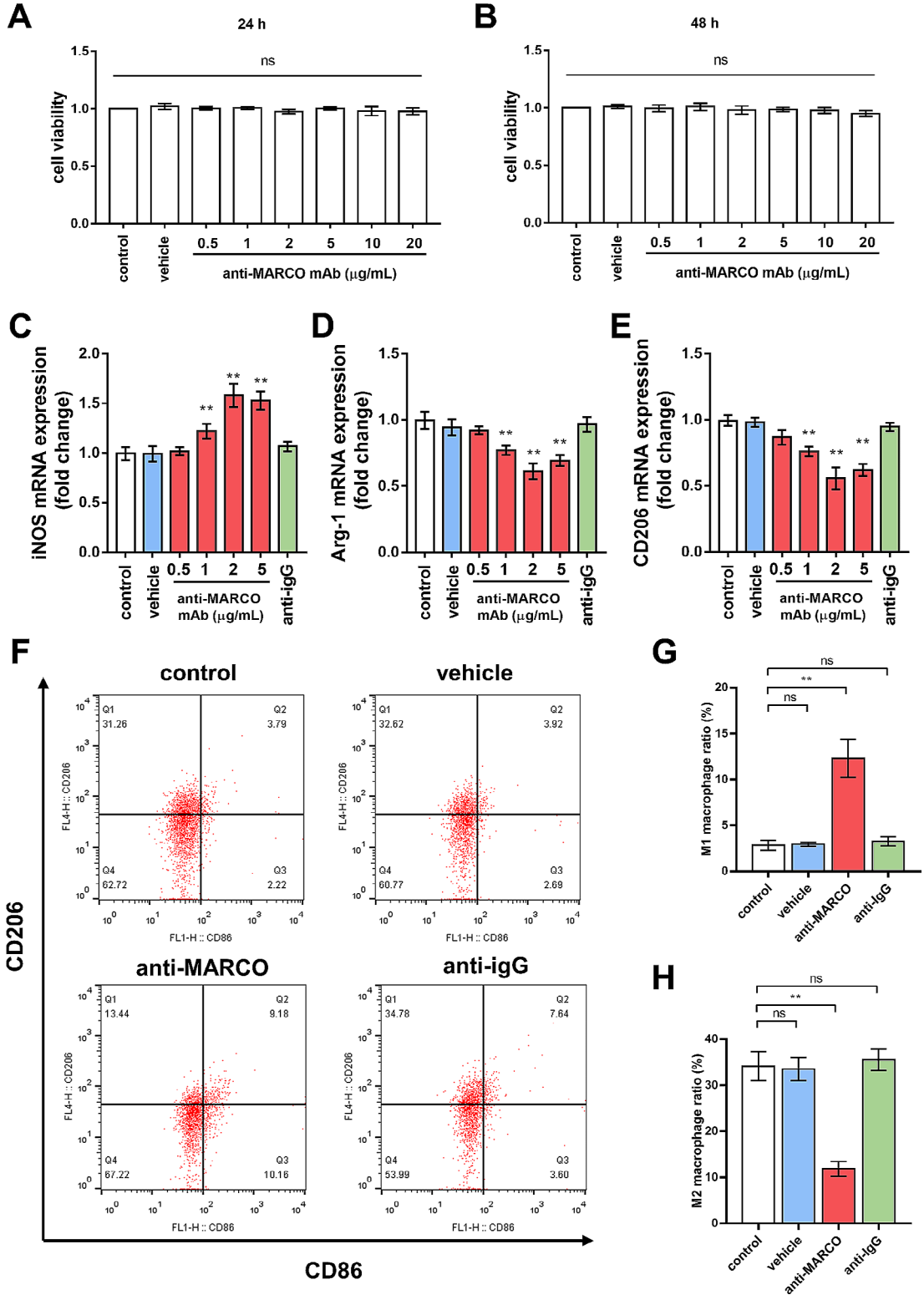

Fig. 1 Effects of Anti-MARCO mAb on macrophages. (**A**-**B**) Effects of exposure to vehicle and different concentrations of anti-MARCO mAb (0.5, 1, 2,5, 10, and 20 μg/mL) on macrophage viability for 24 and 48 h using CCK8. (**C**–**E**) Relative mRNA expression levels of iNOS, Arg-1, and CD206 determined by qPCR. (**F**) Flow cytometry analysis of $CD86^{+}CD206^{-}$ M1 macrophages and $CD86^{-}CD206^{+}$ M2 macrophages. (**G**) Flow cytometry results indicating that $CD86^{+}CD206^{-}$ M1 macrophages increase significantly after anti-MARCO mAb treatment. (**H**) Flow cytometry results indicating that $CD86^{-}CD206^{+}$ M2 macrophages decrease significantly after anti-MARCO mAb treatment. *$p < 0.05$ and **$p < 0.01$. n.s., not significant

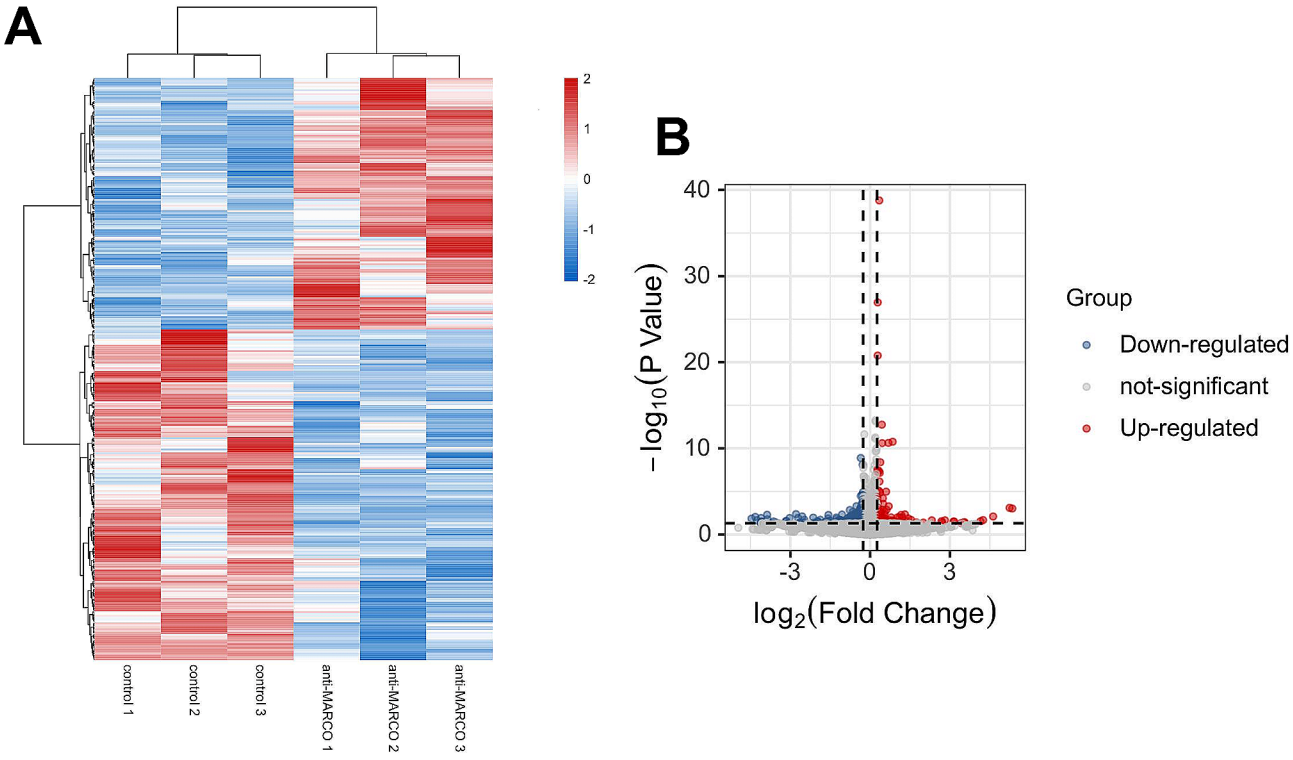

Fig. 2 DEGs analysis. (**A**) The heatmap of DEGs identified by transcriptome sequencing between control and anti-MARCO mAb groups. (**B**) Volcano plot of DEGs

Anti-MARCO mAb exerted an anti-tumor effect by polarizing macrophages from M2 macrophages to M1 macrophages in vitro

This investigation focused on the role of anti-MARCO mAb in treating osteosarcoma. The diagram of the co-culture model is established in Fig. 6A. First, the cell viability was evaluated using the CCK8 assay at 24, 48, and 72 h. The results indicated a significant decrease in viability in the anti-MARCO mAb-treated M2 macrophage group, whereas an increase in cell viability was observed in the M2 macrophage group, indicating that anti-MARCO mAb-treated M2 macrophages can inhibit the viability of U2OS cells (Fig. 6B). The cell scratch test was subsequently performed to study the cell migration. A higher healing rate indicated a stronger cell migration ability.The cell scratch assay demonstrated a significant reduction in the wound healing area in the anti-MARCO mAb-treated M2 macrophage group compared to that in the M2 macrophage group, whereas the M2 macrophage group showed an increase in the wound healing area (Fig. 6C and D). This suggests that anti-MARCO mAb could inhibit tumor cell migration in vitro by influencing macrophage polarization. To determine the impact of anti-MARCO mAb-treated M2 macrophages on U2OS cell apoptosis, the apoptotic ratio of cells was assessed using Annexin V-FITC and PI. The results revealed a significant promotion of apoptosis in U2OS cells co-cultured with anti-MARCO mAb-treated M2 macrophages, indicating that anti-MARCO mAb promoted apoptosis in U2OS cells (Fig. 6E–F). Furthermore, a significant increase in the proportion of U2OS cells in the G0/G1 phase in the anti-MARCO mAb-treated M2 macrophage co-culture was observed by cell cycle distribution analysis, demonstrating that M2 macrophages intervene in the cell cycle and slow down cell division (Fig. 6G–H). In conclusion, anti-MARCO mAb inhibits the growth and migration of osteosarcoma cells in vitro, demonstrating anti-tumor effects.

Discussion

Currently, the 5-year event-free survival rate for patients with non-metastatic osteosarcoma is 60–70%, whereas it is less than 40% for patients with lung metastasis [5]. Consequently, osteosarcoma treatment remains a challenge. In this study, we discovered that anti-MARCO mAb promotes polarization of macrophages toward the M1 macrophage direction, releasing pro-inflammatory factors that induce immune cell activation, thereby inhibiting tumor growth and metastasis and playing an anti-osteosarcoma role. This provides a new approach for osteosarcoma treatment.

Current comprehensive treatment strategies include chemotherapy, surgery, and radiotherapy; however, the prognosis is not optimistic [24–27]. For patients with

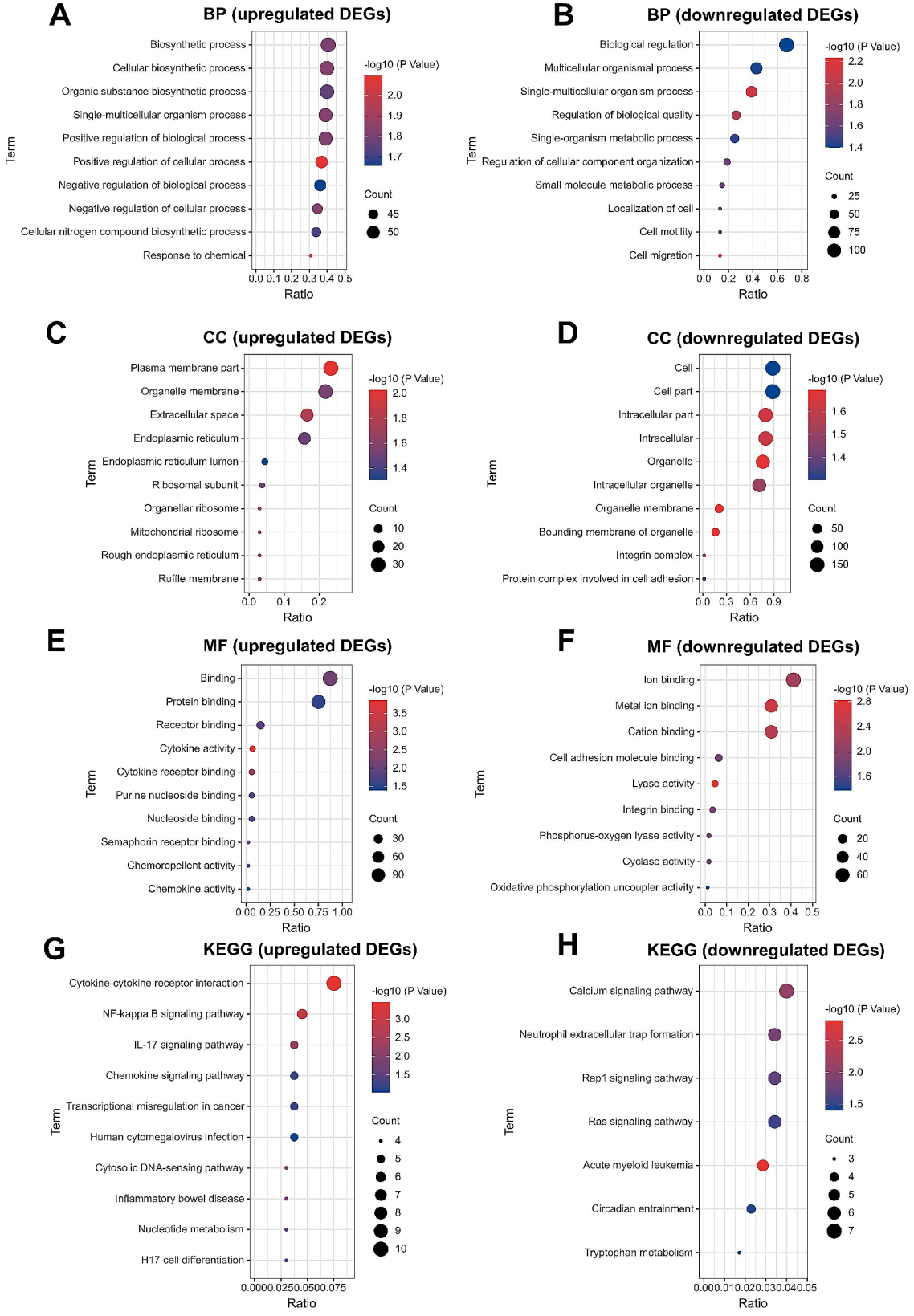

Fig. 3 GO and KEGG enrichment analyses of DEGs. (**A**-**B**) Top 10 BP terms of GO functional annotation of upregulated and downregulated DEGs. (**C**-**D**) Top 10 CC terms of GO functional annotation of upregulated and downregulated DEGs. (**E**-**F**) Top 10 MF terms of GO functional annotation of upregulated and downregulated DEGs. (**G**-**H**) Top 10 enriched KEGG pathways of upregulated and downregulated DEGs. BP: biological process. CC: cellular component. MF: molecular function. KEGG: Kyoto encyclopedia of genes and genomes

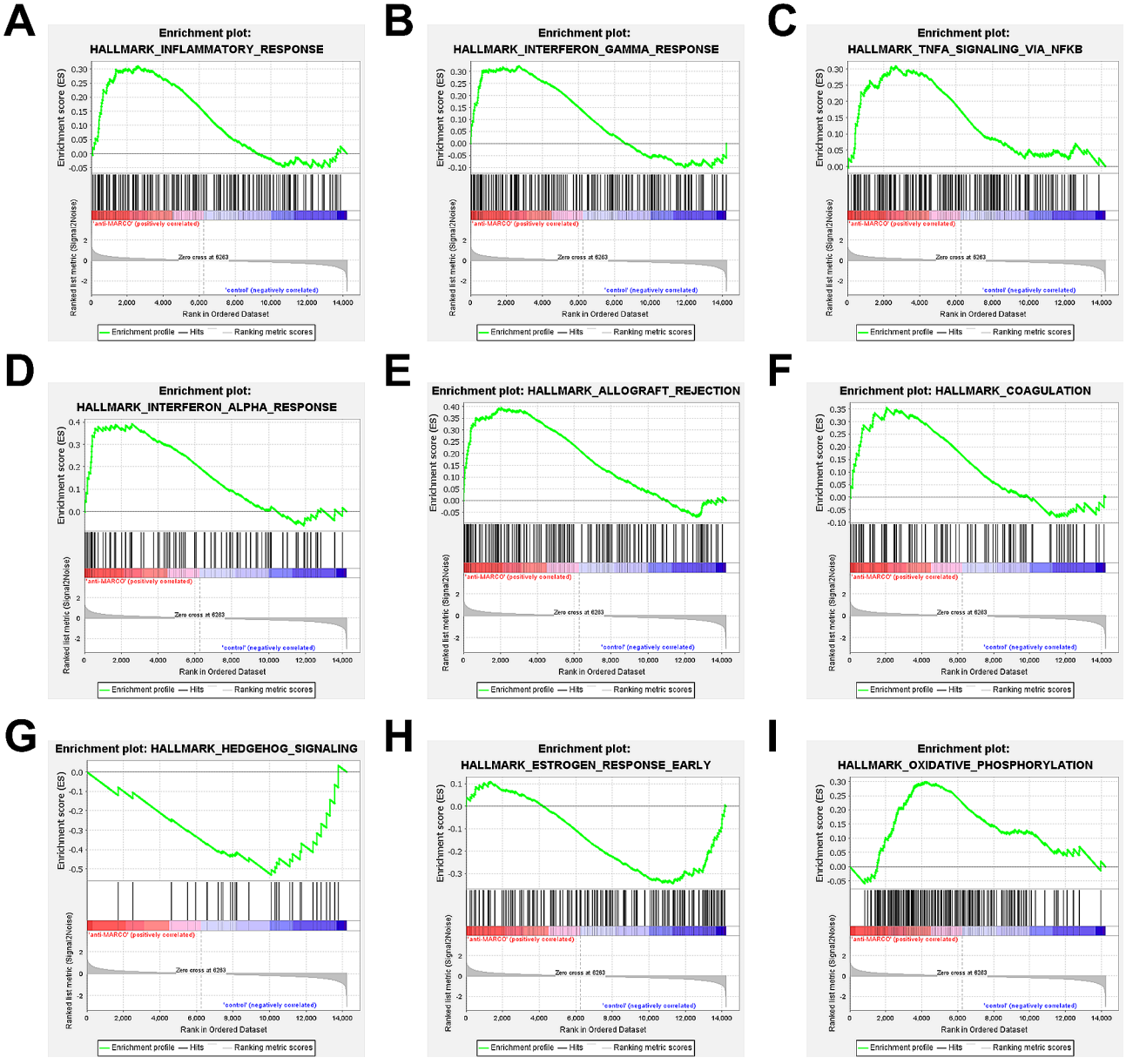

Fig. 4 GSEA of DEGs and analysis of HALLMARK pathways. (**A**) Expression of inflammatory-related gene set. (**B**) Expression of INF-γ-related gene set. (**C**) Expression of TNF-α-signaling-via-NFKβ related gene set. (**D**) Expression of TNF-α-related gene set. (**E**) Expression of allograft rejection-related gene set. (**F**) Expression of coagulation-related gene set. (**G**) Expression of Hedgehog signaling-related gene set. (**H**) Expression of estrogen response early related gene set. (**I**) Expression of oxidative phosphorylation-related gene set

poor responses, postoperative and intensified treatments do not improve long-term prognosis [28]. Additionally, the late toxic effects of chemotherapy can adversely impact the quality of life of patients with osteosarcoma [29]. Emerging immunotherapies, particularly immune checkpoint inhibitors, have been successful in clinical applications. Anti-PD-1/PD-L1 monoclonal antibody pembrolizumab has been approved for treating advanced melanoma and refractory non-small cell lung cancer by the Food and Drug Administration [30]. However, clinical studies targeting PD-L1 in osteosarcoma have yielded disappointing results, attributable to only a subset of osteosarcoma patients exhibiting high PD-L1 expression [31]. Therefore, identifying new therapeutic targets is crucial. Macrophages (M1 and M2) play a significant role in the TME and osteosarcoma [32]. MARCO was initially discovered to be expressed in the TME of invasive breast cancer, correlating with breast cancer progression and recurrence [19]. MARCO+TAMs have been identified in numerous cancer models and are highly expressed in M2 macrophages [33, 34]. Specifically, targeting MARCO has been employed for treating breast cancer,

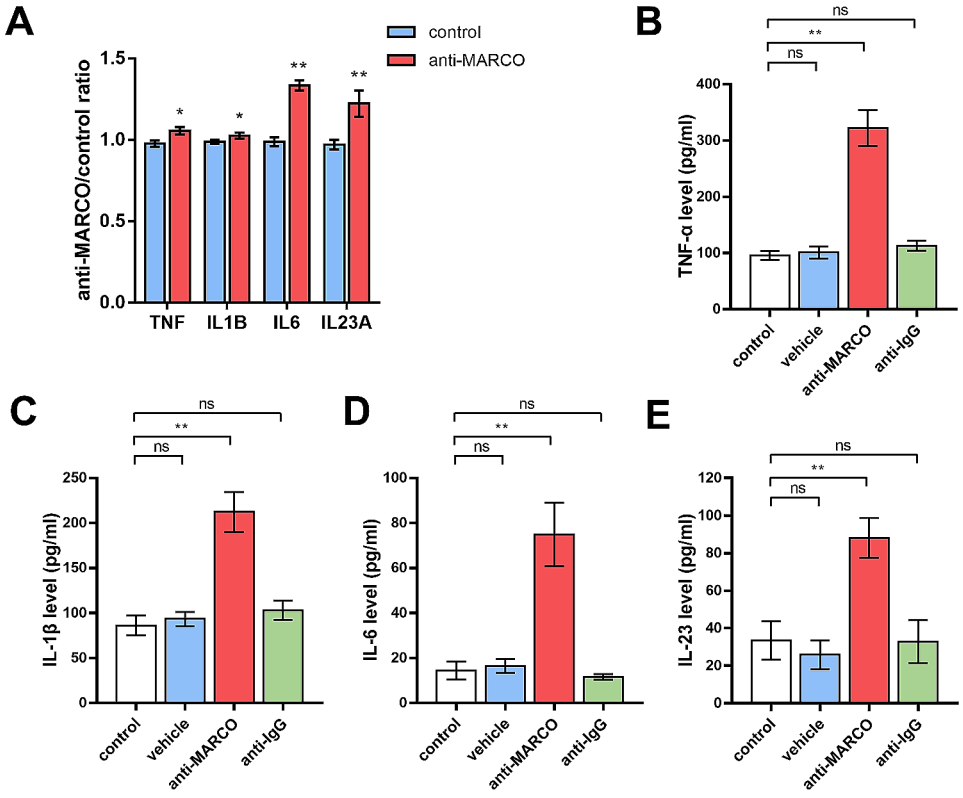

Fig. 5 Anti-MARCO mAb-treated macrophages indicating pro-inflammatory characteristics. (**A**) Anti-MARCO mAb treatment increased the mRNA expression levels of TNF-α, IL-1β, IL-6, and IL-23 in macrophages. (**D**–**G**) The ELISA results showing that anti-MARCO mAb treatment enhances the secretion of TNF-α, IL-1β, IL-6, and IL-23. *$p < 0.05$ and **$p < 0.01$

colorectal cancer, and melanoma, thereby enhancing the therapeutic effects of anti-CTLA4 mAb for melanoma [23]. However, whether specific targeting of MARCO has therapeutic effects in osteosarcoma remains to be investigated. In this study, we first discovered that anti-MARCO mAb at concentrations of 0.5, 1, 2, 5, 10, and 20 μg/mL did not affect macrophage viability. However, it also altered the mRNA expression of iNOS, Arg-1, and CD206. Flow cytometry results also confirmed that anti-MARCO mAb induces polarization of macrophages toward M1 macrophages, indicating that anti-MARCO mAb promotes M1 macrophage polarization. In previous studies, researchers confirmed in rodent models that anti-MARCO mAb can regulate macrophage polarization through a pathway dependent on Fc gamma receptor IIb (FcgRIIb) [23]. Our human cell studies further confirmed that anti-MARCO mAb can regulate macrophage polarization.

M2 macrophages in TAMs allow tumor cells to evade immune responses and promote their growth and metastasis [35]. Simultaneously, tumor cells can regulate the TME through metabolic reprogramming, inducing the transformation of M1 macrophages into M2 macrophages, which is favorable for their growth and dissemination [36, 37]. Previous studies have demonstrated that M1 macrophages, CD8+T cells, and NK cells can maintain an inflammatory state, enabling the immune system to detect and engulf tumor cells [18]. M1 macrophages can kill tumor cells by releasing tumor-killing molecules, including reactive oxygen species [17]. Moreover, M1 macrophages possess robust phagocytic and antigen-presenting capabilities. Bioinformatic analysis revealed that anti-MARCO mAb increased the expression levels of various pro-inflammatory factors. This phenomenon attracts T and B cells to the infection site, preventing tumor cells from evading the immune response [38]. Through bioinformatics analysis, we observed that anti-MARCO mAb induced the polarization of macrophages toward the pro-inflammatory direction, leading to increased secretion of pro-inflammatory factors (TNF-α, IL-1β, IL-6, and IL-23) and upregulation of inflammation-related pathways. ELISA assays also confirmed elevated secretion of the pro-inflammatory factors TNF-α, IL-1β, IL-6, and IL-23. This indicates that the anti-MARCO mAb induces the polarization of macrophages toward the pro-inflammatory direction, thereby exerting an anti-tumor effect.

Finally, the effects of anti-MARCO mAb-treated macrophages on osteosarcoma cells were explored. We observed that it reduced the activity of tumor cells.

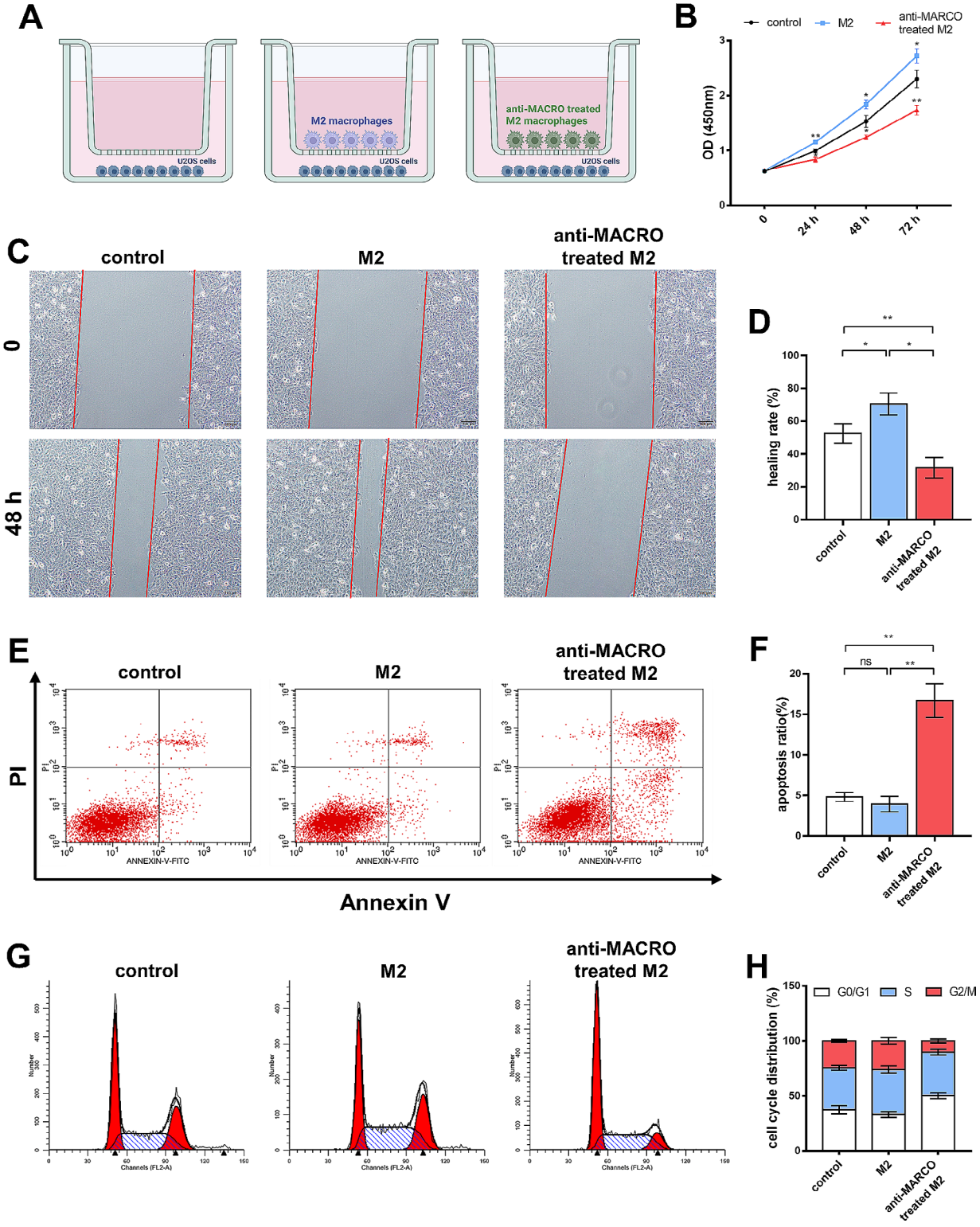

Fig. 6 Effects of anti-MARCO mAb-treated macrophages on U2OS cells. (**A**) Cell co-culture model diagram. (**B**) The CCK8 results showed that the cell viability of U2OS cells was inhibited by anti-MARCO mAb-treated macrophages. (**C**) Representative picture of wound healing assay. (**D**) The wound healing assay results showed that anti-MARCO mAb-treated macrophages significantly reduced the capacity of U2OS cell migration. (**E**) Representative picture of Annexin V/PI double-staining flow cytometry. (**F**) The apoptosis assay results showing that anti-MARCO mAb-treated macrophages significantly promote the U2OS cell apoptosis. (**G**) Representative picture of the cell cycle using flow cytometry with PI staining. (**H**) The cell cycle analysis results showed that anti-MARCO mAb-treated macrophages inhibited the cell cycle progression of U2OS cells. *$p < 0.05$ and **$p < 0.01$

Cell scratch test assays revealed its ability to inhibit the migration of tumor cells, apoptosis assays demonstrated its ability to promote the apoptosis of tumor cells, and cell cycle analysis showed that cells mostly remained in the G0/G1 phase. These results demonstrate the inhibitory effects of anti-MARCO mAb in vitro. Our study demonstrated that anti-MARCO mAb exhibited inhibitory effects on osteosarcoma cells by regulating macrophage polarization in vitro, indicating that anti-MARCO mAb holds potential as a promising therapeutic antibody for osteosarcoma. Monoclonal antibodies currently have a wide range of clinical applications, are used for treating various diseases, including cancer, Alzheimer's disease, and severe infections, and exhibit good specificity [39–41]. Therefore, the anti-MARCO mAb may represent an effective approach for the clinical application of anti-MARCO mAb therapy. Although our study has certain limitations, being limited to in vitro experiments without animal studies and lacking an in-depth exploration of the underlying mechanisms, further research is still required. Nevertheless, our study demonstrated that anti-MARCO mAb can inhibit the growth and metastasis of osteosarcoma cells, providing a new avenue for treating osteosarcoma and its metastasis.

Conclusions

In summary, the current study's findings show that anti-MARCO mAb causes the polarization of macrophages toward M1 macrophages to inhibit osteosarcoma development, indicating that anti-MARCO mAb holds potential as a promising therapeutic antibody for osteosarcoma. The discovery of the anti-osteosarcoma effect of anti-MARCO mAb serves as the basis for determining the roles of targeting MARCO of tumor-associated macrophages in treating osteosarcoma and its potential as a therapeutic agent. Further research is required to explore the clinical applications of anti-MARCO mAb.

Abbreviations

TAM	Tumor-associated macrophages
TME	Tumor microenvironment
PD	L1-Programmed cell death ligand 1
MARCO	Macrophage receptor with collagenous structure
PMA	Phorbol 12-myristate 13-acetate
ELISA	Enzyme-linked immunosorbent assay
GO	Gene ontology
GSEA	Gene set enrichment analysis
CCK	8-CELL Counting Kit-8

Supplementary Information

The online version contains supplementary material available at https://doi.org/10.1186/s13018-024-04950-2.

Supplementary Material 1

Acknowledgements

Not applicable.

Author contributions

ZJ and PH designed the research study. ZJ, LD and YC performed the research. HW, DL and WC analyzed the data. YC wrote the manuscript. All authors contributed to editorial changes in the manuscript. All authors read and approved the final manuscript.

Funding

This work is supported in part by the China Postdoctoral Science Foundation (Grant No. 2023M732295).

Data availability

No datasets were generated or analysed during the current study.

Declarations

Ethics approval and consent to participate

Not applicable.

Consent for publication

Not applicable.

Competing interests

The authors declare no competing interests.

Author details

[1]Department of Orthopedic Surgery, Fudan University Jinshan Hospital, Shanghai, China
[2]Center for Joint Surgery, Department of Orthopedic Surgery, The Second Affiliated Hospital of Chongqing Medical University, Linjiang road No.76, Yuzhong District, Chongqing, China
[3]Department of Orthopedic Surgery, Shanghai Sixth People's Hospital, No.600, Yishan Road, Shanghai, China

Received: 13 May 2024 / Accepted: 25 July 2024
Published online: 31 July 2024

References

1. Ying H, Li ZQ, Li MP, Liu WC. Metabolism and senescence in the immune microenvironment of osteosarcoma: focus on new therapeutic strategies. Front Endocrinol. 2023;14:1217669.
2. Siegel RL, Miller KD, Wagle NS, Jemal A. Cancer statistics, 2023. Cancer J Clin. 2023;73(1):17–48.
3. Mirabello L, Troisi RJ, Savage SA. Osteosarcoma incidence and survival rates from 1973 to 2004: data from the Surveillance, Epidemiology, and end results program. Cancer. 2009;115(7):1531–43.
4. Hayden JB, Hoang BH. Osteosarcoma: basic science and clinical implications. Qld Gov Min J. 2006;37(1):1–7.
5. Gill J, Gorlick R. Advancing therapy for osteosarcoma. Nat Reviews Clin Oncol. 2021;18(10):609–24.
6. Jin J, Cong J, Lei S, Zhang Q, Zhong X, Su Y, Lu M, Ma Y, Li Z, Wang L, et al. Cracking the code: deciphering the role of the tumor microenvironment in osteosarcoma metastasis. Int Immunopharmacol. 2023;121:110422.
7. Beird HC, Bielack SS, Flanagan AM, Gill J, Heymann D, Janeway KA, Livingston JA, Roberts RD, Strauss SJ, Gorlick R, Osteosarcoma. Nat Rev Dis Primers. 2022;8(1):77.
8. Bielack SS, Kempf-Bielack B, Delling G, Exner GU, Flege S, Helmke K, Kotz R, Salzer-Kuntschik M, Werner M, Winkelmann W, et al. Prognostic factors in high-grade osteosarcoma of the extremities or trunk: an analysis of 1,702 patients treated on neoadjuvant cooperative osteosarcoma study group protocols. J Clin Oncology: Official J Am Soc Clin Oncol. 2002;20(3):776–90.
9. Sharma P, Allison JP. The future of immune checkpoint therapy. Sci (New York NY). 2015;348(6230):56–61.
10. Xie L, Xu J, Sun X, Guo W, Gu J, Liu K, Zheng B, Ren T, Huang Y, Tang X et al. Apatinib plus camrelizumab (anti-PD1 therapy, SHR-1210) for advanced osteosarcoma (APFAO) progressing after chemotherapy: a single-arm, open-label, phase 2 trial. J Immunother Cancer 2020, 8(1).

11. Yang C, Tian Y, Zhao F, Chen Z, Su P, Li Y, Qian A. Bone Microenvironment and Osteosarcoma Metastasis. International journal of molecular sciences 2020, 21(19).
12. Fujiwara T, Healey J, Ogura K, Yoshida A, Kondo H, Hata T, Kure M, Tazawa H, Nakata E, Kunisada T et al. Role of Tumor-Associated macrophages in Sarcomas. Cancers 2021, 13(5).
13. Beerling E, Seinstra D, de Wit E, Kester L, van der Velden D, Maynard C, Schäfer R, van Diest P, Voest E, van Oudenaarden A, et al. Plasticity between epithelial and mesenchymal States unlinks EMT from metastasis-enhancing stem cell capacity. Cell Rep. 2016;14(10):2281–8.
14. Zhou J, Tang Z, Gao S, Li C, Feng Y, Zhou X. Tumor-Associated macrophages: recent insights and therapies. Front Oncol. 2020;10:188.
15. Anand N, Peh KH, Kolesar JM. Macrophage repolarization as a therapeutic strategy for Osteosarcoma. Int J Mol Sci 2023, 24(3).
16. Heymann MF, Lézot F, Heymann D. The contribution of immune infiltrates and the local microenvironment in the pathogenesis of osteosarcoma. Cell Immunol. 2019;343:103711.
17. Pan Y, Yu Y, Wang X, Zhang T. Tumor-Associated macrophages in Tumor Immunity. Front Immunol. 2020;11:583084.
18. Basak U, Sarkar T, Mukherjee S, Chakraborty S, Dutta A, Dutta S, Nayak D, Kaushik S, Das T, Sa G. Tumor-associated macrophages: an effective player of the tumor microenvironment. Front Immunol. 2023;14:1295257.
19. Bergamaschi A, Tagliabue E, Sørlie T, Naume B, Triulzi T, Orlandi R, Russnes HG, Nesland JM, Tammi R, Auvinen P, et al. Extracellular matrix signature identifies breast cancer subgroups with different clinical outcome. J Pathol. 2008;214(3):357–67.
20. Gu C, Wiest M, Zhang W, Halder K, Zurawski S, Zurawski G, Joo H, Oh S. Cancer Cells Promote Immune Regulatory Function of Macrophages by upregulating scavenger receptor MARCO Expression. J Immunol. 2023;211(1):57–70.
21. La Fleur L, Boura VF, Alexeyenko A, Berglund A, Pontén V, Mattsson JSM, Djureinovic D, Persson J, Brunnström H, Isaksson J, et al. Expression of scavenger receptor MARCO defines a targetable tumor-associated macrophage subset in non-small cell lung cancer. Int J Cancer. 2018;143(7):1741–52.
22. Chen AX, Gartrell RD, Zhao J, Upadhyayula PS, Zhao W, Yuan J, Minns HE, Dovas A, Bruce JN, Lasorella A, et al. Single-cell characterization of macrophages in glioblastoma reveals MARCO as a mesenchymal pro-tumor marker. Genome Med. 2021;13(1):88.
23. Georgoudaki AM, Prokopec KE, Boura VF, Hellqvist E, Sohn S, Östling J, Dahan R, Harris RA, Rantalainen M, Klevebring D, et al. Reprogramming Tumor-Associated macrophages by antibody targeting inhibits Cancer Progression and Metastasis. Cell Rep. 2016;15(9):2000–11.
24. Tawbi HA, Burgess M, Bolejack V, Van Tine BA, Schuetze SM, Hu J, D'Angelo S, Attia S, Riedel RF, Priebat DA, et al. Pembrolizumab in advanced soft-tissue sarcoma and bone sarcoma (SARC028): a multicentre, two-cohort, single-arm, open-label, phase 2 trial. Lancet Oncol. 2017;18(11):1493–501.
25. Duffaud F, Mir O, Boudou-Rouquette P, Piperno-Neumann S, Penel N, Bompas E, Delcambre C, Kalbacher E, Italiano A, Collard O, et al. Efficacy and safety of regorafenib in adult patients with metastatic osteosarcoma: a non-comparative, randomised, double-blind, placebo-controlled, phase 2 study. Lancet Oncol. 2019;20(1):120–33.
26. Kager L, Zoubek A, Pötschger U, Kastner U, Flege S, Kempf-Bielack B, Branscheid D, Kotz R, Salzer-Kuntschik M, Winkelmann W, et al. Primary metastatic osteosarcoma: presentation and outcome of patients treated on neoadjuvant Cooperative Osteosarcoma Study Group protocols. J Clin Oncology: Official J Am Soc Clin Oncol. 2003;21(10):2011–8.
27. Seidensaal K, Mattke M, Haufe S, Rathke H, Haberkorn U, Bougatf N, Kudak A, Blattmann C, Oertel S, Kirchner M, et al. The role of combined ion-beam radiotherapy (CIBRT) with protons and carbon ions in a multimodal treatment strategy of inoperable osteosarcoma. Radiotherapy Oncology: J Eur Soc Therapeutic Radiol Oncol. 2021;159:8–16.
28. Bielack SS, Smeland S, Whelan JS, Marina N, Jovic G, Hook JM, Krailo MD, Gebhardt M, Pápai Z, Meyer J, et al. Methotrexate, Doxorubicin, and cisplatin (MAP) plus maintenance Pegylated Interferon Alfa-2b versus MAP alone in patients with Resectable High-Grade Osteosarcoma and good histologic response to preoperative MAP: first results of the EURAMOS-1 Good Response Randomized Controlled Trial. J Clin Oncology: Official J Am Soc Clin Oncol. 2015;33(20):2279–87.
29. Edelmann MN, Daryani VM, Bishop MW, Liu W, Brinkman TM, Stewart CF, Mulrooney DA, Kimberg C, Ness KK, Cheung YT, et al. Neurocognitive and patient-reported outcomes in adult survivors of Childhood Osteosarcoma. JAMA Oncol. 2016;2(2):201–8.
30. Kwok G, Yau TC, Chiu JW, Tse E, Kwong YL. Pembrolizumab (Keytruda). Hum Vaccines Immunotherapeutics. 2016;12(11):2777–89.
31. Shen JK, Cote GM, Choy E, Yang P, Harmon D, Schwab J, Nielsen GP, Chebib I, Ferrone S, Wang X, et al. Programmed cell death ligand 1 expression in osteosarcoma. Cancer Immunol Res. 2014;2(7):690–8.
32. Baghban R, Roshangar L, Jahanban-Esfahlan R, Seidi K, Ebrahimi-Kalan A, Jaymand M, Kolahian S, Javaheri T, Zare P. Tumor microenvironment complexity and therapeutic implications at a glance. Cell Communication Signaling: CCS. 2020;18(1):59.
33. Shi B, Chu J, Huang T, Wang X, Li Q, Gao Q, Xia Q, Luo S. The scavenger receptor MARCO expressed by Tumor-Associated macrophages are highly Associated with Poor Pancreatic Cancer Prognosis. Front Oncol. 2021;11:771488.
34. Ding L, Qian J, Yu X, Wu Q, Mao J, Liu X, Wang Y, Guo D, Su R, Xie H, et al. Blocking MARCO(+) tumor-associated macrophages improves anti-PD-L1 therapy of hepatocellular carcinoma by promoting the activation of STING-IFN type I pathway. Cancer Lett. 2024;582:216568.
35. Mantovani A, Allavena P, Sica A, Balkwill F. Cancer-related inflammation. Nature. 2008;454(7203):436–44.
36. Li M, He L, Zhu J, Zhang P, Liang S. Targeting tumor-associated macrophages for cancer treatment. Cell Bioscience. 2022;12(1):85.
37. Bonuccelli G, Avnet S, Grisendi G, Salerno M, Granchi D, Dominici M, Kusuzaki K, Baldini N. Role of mesenchymal stem cells in osteosarcoma and metabolic reprogramming of tumor cells. Oncotarget. 2014;5(17):7575–88.
38. Allavena P, Sica A, Solinas G, Porta C, Mantovani A. The inflammatory microenvironment in tumor progression: the role of tumor-associated macrophages. Crit Rev Oncol/Hematol. 2008;66(1):1–9.
39. Neațu M, Covaliu A, Ioniță I, Jugurt A, Davidescu EI, Popescu BO. Monoclonal Antibody Therapy in Alzheimer's Disease. Pharmaceutics 2023, 16(1).
40. Rocco D, Della Gravara L, Battiloro C, Palazzolo G, Gridelli C. Recently approved and emerging monoclonal antibody immune checkpoint inhibitors for the treatment of advanced non-small cell lung cancer. Expert Opin Biol Ther. 2023;23(3):261–8.
41. de Jong HK, Grobusch MP. Monoclonal antibody applications in travel medicine. Tropical diseases. Travel Med Vaccines. 2024;10(1):2.

Publisher's Note